

Are Automated Molecular Dynamics Simulations and Binding Free Energy Calculations Realistic Tools in Lead Optimization? An Evaluation of the Linear Interaction Energy (LIE) Method

Eva Stjernschantz,^{†,‡} John Marelius,[‡] Carmen Medina,[‡] Micael Jacobsson,^{‡,§}
Nico P. E. Vermeulen,[†] and Chris Oostenbrink^{*,†}

Leiden/Amsterdam Center for Drug Research, Division of Molecular Toxicology, Vrije Universiteit Amsterdam, De Boelelaan 1083, 1081 HV Amsterdam, The Netherlands, Department of Chemistry, Biovitrum AB, SE-112 76 Stockholm, Sweden, and Department of Medicinal Chemistry, Faculty of Pharmacy, University of Uppsala, Box 574, SE-751 23 Uppsala, Sweden

Received April 4, 2006

An extensive evaluation of the linear interaction energy (LIE) method for the prediction of binding affinity of docked compounds has been performed, with an emphasis on its applicability in lead optimization. An automated setup is presented, which allows for the use of the method in an industrial setting. Calculations are performed for four realistic examples, retinoic acid receptor γ , matrix metalloprotease 3, estrogen receptor α , and dihydrofolate reductase, focusing on different aspects of the procedure. The obtained LIE models are evaluated in terms of the root-mean-square (RMS) errors from experimental binding free energies and the ability to rank compounds appropriately. The results are compared to the best empirical scoring function, selected from a set of 10 scoring functions. In all cases, good LIE models can be obtained in terms of free-energy RMS errors, although reasonable ranking of the ligands of dihydrofolate reductase proves difficult for both the LIE method and scoring functions. For the other proteins, the LIE model results in better predictions than the best performing scoring function. These results indicate that the LIE approach, as a tool to evaluate docking results, can be a valuable asset in computational lead optimization programs.

INTRODUCTION

Automated flexible docking is a widely used tool for binding mode prediction and binding affinity estimation in lead optimization projects as well as in virtual screening for new compounds. While sampling the flexibility of the ligand, the protein is usually kept rigid during docking. A well-known weakness of docking therefore concerns protein conformational changes upon ligand binding, that is, induced fit, which to a large extent cannot be accounted for using current docking algorithms.¹ In addition, mobile water molecules are usually disregarded in docking for sampling reasons. Structurally well-defined water molecules can be included but are in most cases kept fixed throughout the docking procedure. The inclusion of rigid water molecules in docking calculations has been applied successfully in previous studies² but could be unfavorable when docking a set of diverse ligands, particularly if the water molecules are directly interacting with the ligand. For binding affinity prediction, docking programs rely on relatively simple empirical or knowledge-based scoring functions.³ In addition to accurate binding mode prediction and the ability to discriminate between binders and nonbinders in a virtual ligand screening approach, scoring functions should be able to accurately rank binders according to binding affinity. Several studies have shown that scoring functions generally

perform poorly in this aspect.^{4,5} Empirical scoring functions are often biased toward the training set that has been used for parametrization.^{3,4} Different scoring functions usually display weaknesses in describing different properties of the system. Studies to identify the best scoring function for different targets show that no single scoring function performs well for diverse targets and ligand sets.^{5,6} Correlations of docking scores with ligand properties such as molecular weight have also been described.⁷

During lead optimization, chemical libraries containing 10–100 compounds are designed. In a typical industrial project, one or a few crystal structures of the protein of interest might be available, but the number of molecules to be studied always exceeds the available structural information. The current simplifications implicit in the docking method do not allow for an accurate description of the protein–ligand–water interactions and, thus, the free energy of binding. Detailed molecular dynamics (MD) simulations are needed for this but require a good initial structure of the bound ligands. If the binding poses from a docking experiment are sufficiently good, they could be used as starting points for MD simulations to calculate a more accurate free energy of binding. This might result in better ranking of the compounds than with the simple scoring functions of the docking tools. Molecular dynamics is, however, a computationally rather expensive method, and setting up the simulations as well as analyzing the results can be elaborate.⁸ Relative free energies of binding for several ligands to a common protein can be calculated using free-energy pertur-

* Corresponding author phone: +31 20 5987606; fax: +31 20 5987610; e-mail: c.oostenbrink@few.vu.nl.

[†] Vrije Universiteit Amsterdam.

[‡] Biovitrum AB.

[§] University of Uppsala.

bation (FEP) methods,^{9,10} but these are currently too time-consuming to use in a high-throughput setup and are thus not efficient tools for lead optimization.¹¹

For the prediction of the binding free energy, Åqvist et al. introduced the linear interaction energy (LIE) method.¹² The LIE method is a semiempirical method, based on linear response theory, which is less computationally expensive than FEP calculations but more accurate than scoring functions.¹¹ See below for a detailed description of the LIE method.

In an attempt to fill the gap between the docking and scoring of a large number of compounds, on one hand, and elaborate molecular dynamics simulations and FEP calculations applied on very few compounds, on the other, we investigate the possibility of using molecular dynamics simulations in a semi-high-throughput fashion using the LIE method for binding free energy prediction in lead optimization. The aim of this study is to investigate (1) the dependence of free energy calculations on the initial structure used for MD, (2) if the free energies of binding from MD give a substantially better ranking of the compounds than the simple scoring functions, and (3) if such a setup could be useful in a real industrial project.

A number of docking–scoring evaluation studies have been described recently,^{3–5,13–16} but similar extensive tests of the more elaborate methods, such as FEP and LIE, have not yet been performed. Previous studies of the LIE method's performance on single targets with relatively small ligand sets indicate that a root-mean-square (RMS) error from the experimental binding free energy of less than ~1 kcal/mol can be expected if the LIE model is reparametrized for each target/ligand set.^{17–22} In extensive studies of the performance of scoring functions, the best results in terms of RMS errors from experimental binding free energies are in the range of 2–2.5 kcal/mol.¹⁴ It should be noted that, for the application described here, an accurate ranking of compounds is more important than an accurate prediction of the values of the binding free energies in itself.

To apply the LIE method in real-life lead optimization programs, an automated setup to run and analyze molecular dynamics simulations from docked protein–ligand complexes was constructed. For the evaluation of the LIE method, four targets displaying different binding site properties were chosen: retinoic acid receptor γ (RAR γ), matrix metalloprotease 3 (MMP-3), estrogen receptor α (ER α), and dihydrofolate reductase (DHFR). Each of these real-case examples addresses specific aspects of the approach. The targets and ligand sets that were used are presented in Table 1 and Figure 1. Structures of all of the ligands are available in the Supporting Information.

RAR γ was used to evaluate the significance of the docking accuracy for the molecular dynamics setup and the LIE method. Seven crystallographic complexes of RAR γ with different ligands were used, and simulations were started from the crystal structure conformations. In addition, the seven ligands were docked to one of the crystal structures, and the docked ligand conformations were used as starting structures for a second set of MD simulations. Two LIE models were constructed and compared.

MMP-3, ER α , and DHFR were used to evaluate the LIE method with large sets of ligands for each target^{23–26} docked to one crystallographic complex structure. The docked compounds were rescored with 10 scoring functions, and the

Table 1. Summary of the Targets and Ligand Sets Used for the Evaluation of the Automated LIE Method^a

target	PDB ID	number of ligands	number of ligands training set	number of ligands test set	ligand source
RAR γ	1EXA	7 ^b			Klaholz ³⁶
MMP-3	1HY7	54	27	27	Ha ²³
ER α	1ERE	36	18	18	Sippl ²⁴
DHFR	1RX3	29	14	15	Otzen ²⁵
DHFR	1RX3	12		12	Zolli-Juran ²⁶

^a RAR γ : retinoic acid receptor γ . MMP-3: matrix metalloprotease 3. ER α : estrogen receptor α . DHFR: dihydrofolate reductase. The PDB ID corresponds to the crystal structure used for docking. For RAR γ , the ligands were not split into training and test sets because of the size of the ligand set. The Zolli-Juran compounds were used as an additional test set for the DHFR model. ^b Ligands from different crystallographic complexes docked to one of the crystal structures.

best performing scoring function for each target was selected. The performance of this scoring function was compared to that of the LIE method. MMP-3 and ER α represent two extremes in terms of binding site properties. The binding site of MMP-3 is large, open toward the solvent, and contains a zinc ion, which directly participates in ligand binding.²⁷ The ligand-binding pocket of ER α is small, closed, and rather hydrophobic, typically binding rigid steroidlike compounds, and displays only a few hydrogen-bond possibilities.²⁸ The two binding sites are depicted in Figure 2. The most challenging protein target was DHFR. Two sets of ligands, one from the same chemical series²⁵ and one from a different set, originating from hits of a high-throughput screen,²⁶ were docked to a DHFR complex crystal structure.²⁹ Different LIE models were constructed to estimate the applicability of LIE models parametrized on one series of ligands to other sets of ligands for the same target as well as the quality of LIE models constructed on a diverse set of ligands.

THEORETICAL BACKGROUND

FEP calculations rely on the simulation of several different states—mostly unphysical—between two different ligands, from which estimates of their relative binding affinities can be obtained. In contrast, the LIE approach uses only the initial and final states of the binding process of one ligand, that is, the free and bound states of the ligand. Two simulations are performed: the ligand in water and the ligand in complex with solvated protein (from here on denoted as the “free simulation” and the “protein simulation”, respectively).³⁰ The binding free energy is given by

$$\Delta G_{\text{bind}} = \Delta G_{\text{sol}}^{\text{p}} - \Delta G_{\text{sol}}^{\text{w}} \quad (1)$$

where “sol” denotes the solvation free energy change of transferring the ligand from the gas phase to the different environments “p” (protein) and “w” (water). The solvation free energies are calculated as the sum of intermolecular electrostatic interactions and intermolecular van der Waals interactions between the ligand and its surroundings. The LIE equation can then be written as

$$\Delta G_{\text{bind}} = \beta \Delta \langle V^{\text{el}} \rangle + \alpha \Delta \langle V^{\text{vdW}} \rangle \quad (2)$$

where $\langle \rangle$ denotes the ensemble average and the Δ corre-

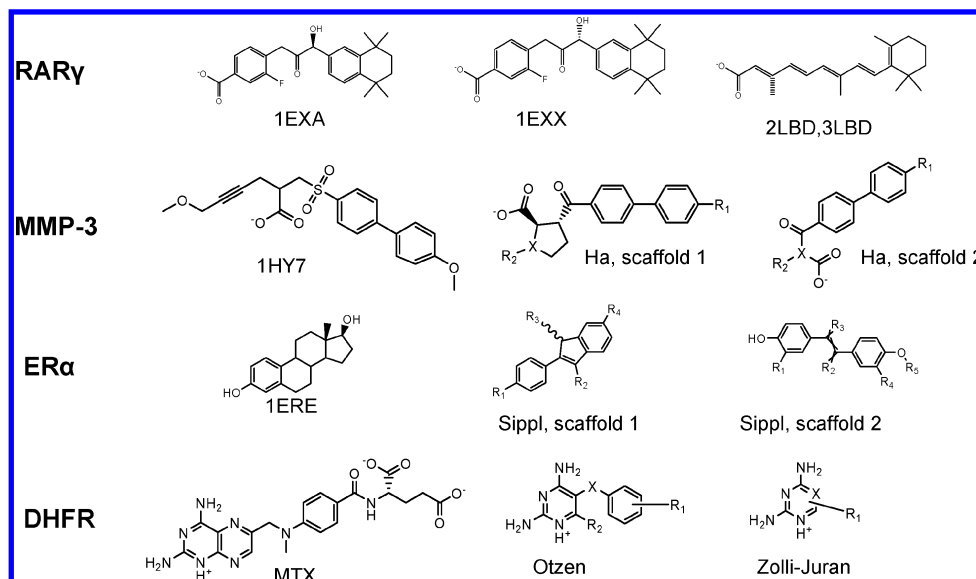


Figure 1. Structures of the cocrystallized ligands of the protein structures used for docking for all four protein targets in this study (left column). RAR γ : The ligand of the crystal structure, PDB code: 1EXX; the inactive stereoisomer of the complex with PDB code 1EXA is also shown as well as two other cocrystallized RAR γ ligands, all-trans and 9-cis retinoic acid, that were used. MMP-3: The 54 docked compounds are represented by two different scaffolds. ER α : The two scaffolds depicted represent 70% of the compounds. Also included in the data set are, e.g., coumestrol, genistein, bisphenol A, estrone, and 17 α - and 17 β -estradiol. In scaffold 1, R₁ and R₄ represent OH or H. In scaffold 2, R₁ and R₄ represent OH, H, or OCH₃. R₂ and R₃ are alkyl chains in both scaffolds. The chiral center described in the text is indicated in scaffold 1. The crossed bonds in scaffold 2 correspond to either a single or a double bond. DHFR: The Otzen compounds all share the scaffold displayed. R₁ is in some cases a benzyl group. Seven of the 11 Zolli-Juran compounds are represented by the depicted scaffold. X is in one case N, but otherwise it is C. In a majority of compounds, R₁ is a benzyl or cyclohexyl group. All of the ligand structures can be found in the Supporting Information.

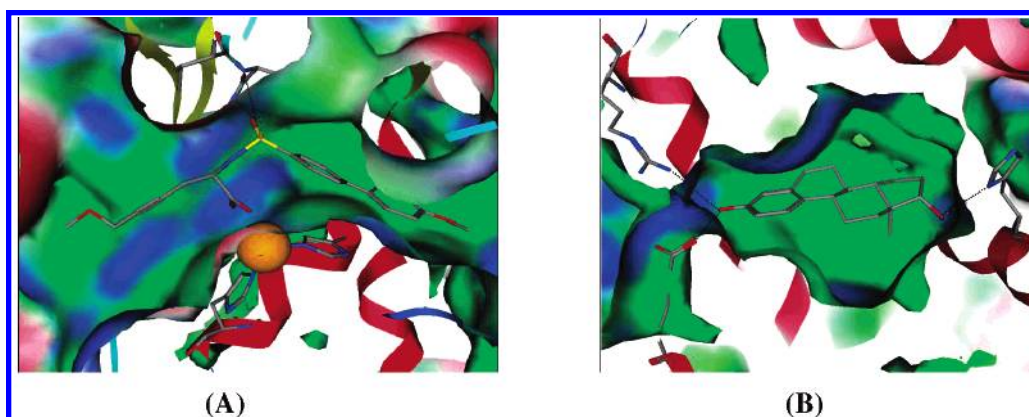


Figure 2. Binding pockets of MMP-3 and ER α . Protein surfaces colored according to the following: hydrophobic residues (green), hydrophilic residues (blue), and exposed residues (red). (A) The binding pocket of MMP-3 is large, partly open toward the solvent, and includes a catalytic zinc ion (displayed in orange), interacting with the ligand. The sulfonamide oxygen of the 1HY7 ligand also forms hydrogen bonds with the backbone of Leu164 and Ala165. The biphenyl moiety fits into the S1' pocket, while the S2 pocket is larger and more exposed. (B) ER α has a closed, mainly hydrophobic pocket with only a few hydrogen-bond possibilities. The substrate, estradiol, forms a hydrogen-bond network with Arg394, Glu353, and a water molecule (not shown). On the opposite side of the pocket, estradiol forms an additional hydrogen bond with His524.

sponds to the difference of these ensemble averages in protein and in water, for example, for the electrostatic interaction energy: $\Delta\langle V^{\text{el}} \rangle = \langle V^{\text{el}} \rangle_{\text{p}} - \langle V^{\text{el}} \rangle_{\text{w}}$.³⁰ Originally, the LIE method was based on the linear response approximation to estimate the electrostatic parts of the solvation free energies, corresponding to a β of $1/2$.¹² Further development of the LIE model showed that improved models could be obtained for a diverse set of systems if the electrostatic part of the free energy was weighted with an empirical β , which was allowed to deviate from $1/2$.¹⁷ Applying different β 's for different sets of ligands, depending on the charge and polar properties of the ligand, has also been described.¹⁷ It has also been shown that, for some systems, a constant γ needs to be added in order to obtain reasonable binding free energy

predictions.²⁰ The LIE equation is thus often used as

$$\Delta G_{\text{bind}} = \beta \Delta \langle V^{\text{el}} \rangle + \alpha \Delta \langle V^{\text{vdW}} \rangle + \gamma \quad (3)$$

A closer examination of the derivation of the linear interaction energy method results in a generalized form, which can be written as

$$\begin{aligned} \Delta G_{\text{bind}} = & \beta_{\text{prot}} \langle V_{1-s}^{\text{el}} \rangle_{\text{prot}} - \beta_{\text{wat}} \langle V_{1-s}^{\text{el}} \rangle_{\text{wat}} + \\ & \alpha_{\text{prot}} \langle V_{1-s}^{\text{vdW}} \rangle_{\text{prot}} - \alpha_{\text{wat}} \langle V_{1-s}^{\text{vdW}} \rangle_{\text{wat}} + \gamma + \delta_1 (\langle V_{1-l}^{\text{el}} \rangle_{\text{prot}} - \\ & \langle V_{1-l}^{\text{el}} \rangle_{\text{wat}}) + \delta_2 (\langle V_{1-l}^{\text{vdW}} \rangle_{\text{prot}} - \langle V_{1-l}^{\text{vdW}} \rangle_{\text{wat}}) \end{aligned} \quad (4)$$

where $l-s$ describes the ligand-surrounding interaction energies and $\langle V_{l-1}^{\text{el}} \rangle$ and $\langle V_{l-1}^{\text{vdW}} \rangle$ are the electrostatic and van der Waals intramolecular ligand interaction energies, also referred to as strain energy. The linear relation between V^{vdW} and a free energy through the parameters α_{prot} and α_{wat} relies on an assumed linear dependence of both energetic terms on a parameter describing the size of the ligand, for example, the solvent-accessible surface area. In cases where this somewhat ad hoc assumption does not hold, the inclusion of the V_{l-1} terms may correct for a difference in ligand shape in the free and protein-bound simulations. For a complete derivation and a description of the underlying assumptions of eq 4, we refer to the Supporting Information. In this study, we obtained the best results with the lowest number of empirical parameters using

$$\Delta G_{\text{bind}} = \beta \Delta \langle V^{\text{el}} \rangle + \alpha \Delta \langle V^{\text{vdW}} \rangle + \delta \Delta (\langle V_{l-1}^{\text{el}} \rangle + \langle V_{l-1}^{\text{vdW}} \rangle) \quad (5)$$

METHODS

Docking Calculations. All docking calculations were performed with GlideSP3.5.^{31–33} The crystal structures used for docking to the four different targets according to their PDB codes³⁴ were as follows: 1EXA³⁵ for the RAR γ ligands, 1HY7²⁷ for the MMP3 ligand set, 1ERE²⁸ for the ER α ligand set, and 1RX3²⁹ for the DHFR ligands. Seven crystal structures were used for calculations on RAR γ : 1EXA,³⁵ 1EXX,³⁵ 1FCX,³⁶ 1FCY,³⁶ 1FCZ,³⁶ 2LBD,³⁷ and 3LBD.³⁸ Ligands were prepared using LigPrep,³³ that is, conversion to 3D and the generation of different protonation states, stereoisomers, and tautomers, followed by minimization. The protein preparations were performed using the Glide protein preparation package. This involves a protonation state determination of the protein, hydrogen addition, and restrained minimization of the protein using the OPLS-AA force field.^{31–33} All water molecules were removed from the protein structures, except for the water molecule in the ER α structure known to be directly involved in ligand binding.²⁸ The catalytic Zn ion in the MMP-3 structure was included as well as the cofactor of DHFR. For each compound, the five best docking poses were saved and the best docking pose was selected by visual inspection and used as starting structure for the molecular dynamics simulations.

MD Simulations. The automated setup of the molecular dynamics simulation of the docked compounds is described in Figure 3. Except for the protein preparation, all steps in this scheme were fully automated and require no human input. All simulations were performed using the program Q.³⁹ Ligand conformations selected from the docking studies were used as starting structures for MD simulations, using Q and the OPLS2001-AA force field parameter set.⁴⁰ Ligand parameters were obtained using Impact.³³ Two simulations were carried out: one of the ligand in water (“free simulation”) and another of the ligand bound to the solvated protein (“protein simulation”). The protein conformation used in the docking calculation was used as the starting structure for the MD simulations. Simulations were carried out in solvated 18 Å (MMP-3) and 20 Å (ER α , RAR γ , and DHFR) simulation spheres. Charged amino acids outside the simulation sphere boundary and within 2–4 Å of the boundary were neutralized. The net charge of the protein was zero in

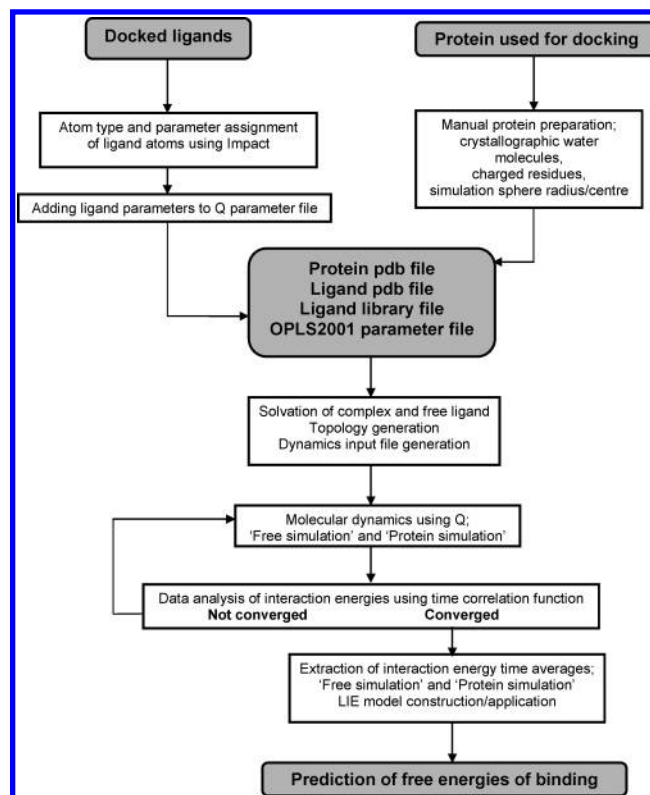


Figure 3. Scheme of the automated setup for molecular dynamics simulations and binding free energy calculations using docked protein–ligand structures as starting conformations. Except for the manual protein preparation, all steps in this scheme have been automated.

all cases. An electrostatic correction term for these neutralized charges was added to the calculated binding free energy, according to eq 6.¹⁸

$$\Delta \Delta G_{\text{el_corr}} = \frac{1}{4\pi\epsilon_0} \sum_{\substack{p \in \text{neutralized ionic residues} \\ l \in \text{ligand atoms}}} \frac{q_p q_l}{r_{p-l}} \quad (6)$$

where q_p is the formal charge of the residue that has been neutralized, q_l is the partial charge of the ligand atom, ϵ is the dielectric constant which was set to 80, and r_{p-l} is the distance between the ligand atom and a central atom of the charged group of the residue. After 20 ps of equilibration, data collection for 375 ps of simulation was performed with a time step of 1.5 fs. Energies were stored for later analysis every 10 steps. The nonbonded list was updated every 50 steps, and the LRF Taylor expansion of the electrostatic field beyond the cutoff radius (10 Å) was calculated. The convergence of interaction energies was checked by ensuring that the autocorrelation function was approaching zero after time intervals corresponding to 50% of the overall simulation time. Systems with insufficient convergence were simulated an additional 200–250 ps. The temperature was maintained at 300 K by coupling to an external bath with a relaxation time of 100 fs.⁴¹ Position restraints on specific residues were applied during the simulations. This should be considered to be part of the protein setup and needs to be investigated before simulating a set of ligands. The same restraints are then applied to all of the protein–ligand simulations of a system. Arg274 in RAR γ was restrained, to avoid its displacement toward the binding site and the ligand car-

boxylate group during simulation. The positioning of Arg274 toward the binding pocket is not observed in any of the RAR γ crystal structures used. Incomplete solvation of the protein, resulting in insufficient shielding of the charges, could be the reason for this simulation artifact. Four histidine residues coordinating the two zinc ions in MMP-3 were restrained to keep them from collapsing into the ions. In ER α , restraints were applied to Arg394 and Glu353 to avoid direct interaction between them and displacement of the bridging water molecule, which was considered to be incorrect. The results of the MMP-3 LIE model are based on simulations with the zinc ion parametrized as a sphere with a charge of +2. In DHFR, the negatively charged terminal phosphate group of NADPH was situated far away from the simulation sphere center and therefore neutralized.

DATA ANALYSIS

The ligand sets were divided into training and test sets of equal size and range in experimental binding free energy.

Scoring Results. The scoring functions implemented in Glide, Glide Score, and Emodel^{31–33} were applied to the docking results. Furthermore, the docked conformations were rescored with the scoring functions available in the Cscore^{42,43} (FlexX-Score,⁴⁴ GOLD-Score,⁴⁵ PMF-Score,⁴⁶ DOCK-Score,⁴⁷ and Chem-Score⁴⁸) and Xscore (HP-Score, HM-Score, and HS-Score)¹⁴ modules. To select the best performing scoring function for each target and compare the scoring with the LIE model, the scores of the training set were correlated with the experimental binding free energy using linear regression. Although a number of the scoring functions included in this study yield binding affinities, this is not the case for all of the scoring functions studied. To obtain a fair comparison of the scoring functions, linear regression was applied to all of them, which should positively bias the scoring function results. The RMS errors of the calculated binding free energies from the experimental binding free energies was calculated for each scoring function. For a comparison of the accuracy of the ranking of ligands, the Spearman rank correlation coefficient was calculated, which should be a better measure for ranking than RMS errors or r^2 .

LIE Model. Ligand-surrounding interaction energies were extracted, and convergence was determined using the time-correlation function. Time averages were calculated for the ligand-surrounding and ligand–ligand intramolecular van der Waals and electrostatic interaction energies. The electrostatic correction terms were calculated according to eq 6 and added to the total calculated binding free energy.¹⁸ The LIE equation was parametrized using the training set and subsequently applied to the test set. Different LIE models were constructed on the basis of the expanded LIE model (eq 4). The best model was selected on the basis of the RMS error from experimental binding free energies, using as few parameters as possible.

RESULTS

Docked Conformations as Starting Structures for MD Simulations. RAR γ was used to evaluate the dependence of docking for the generation of initial structures on the molecular dynamics setup and the LIE method. Seven crystallographic complexes were used,³⁶ and simulations were

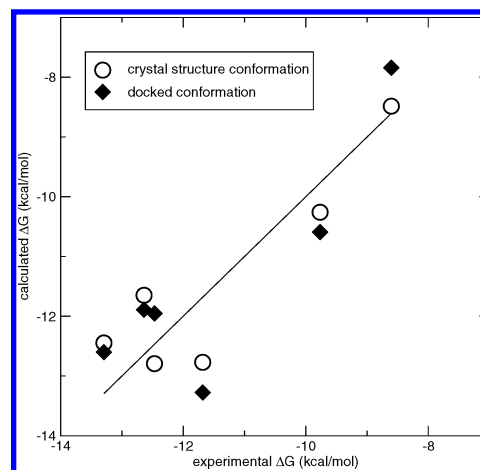


Figure 4. Results of two LIE models based on MD simulations using the RAR γ crystal structure and docked conformations as starting structures; experimental binding free energies are compared to predicted binding free energies. The value for the 1EXX ligand is not displayed, as no experimental value is available. The solid line represents the ideal case.

started from the crystal structure conformation as well as from docked ligand conformations, docked to one of the seven structures. LIE models for the two data sets were constructed using eq 2 and compared. The RAR γ ligand binding site is a closed pocket, characterized by a hydrogen-bond network at the inner end, formed by Arg278, Ser289, Leu233, and a water molecule. Elsewhere, the binding site is mainly constituted of hydrophobic residues.³⁵ All of the crystallized ligands are anchored with a carboxylate group to the inner end of the pocket through the hydrogen-bond network. Figure 1 displays examples of the cocrystallized ligands used in this study. Docking results of the ligands to the 1EXA structure were generally good, with RMS deviations of less than 1 Å from the ligand binding mode of the corresponding crystal structures. Figure 4 displays the calculated binding free energies applying the two LIE models, based on MD simulations starting from crystal structures and docked conformations, respectively. Values of α and β in the two LIE models and RMS errors from the experimental binding free energies are shown in Table 2. The LIE crystal structure model is shown to be slightly better than the LIE model based on docked conformations, as seen from the RMS errors of 0.74 and 0.92 kcal/mol, respectively, which is to be expected. However, the latter model is similar to the model based on the crystal structures in terms of α and β values. It should be noted that the docking solutions in this case were very good. In both RAR γ LIE models, the ligand of the 1EXX crystal structure, see Figure 1, is correctly predicted to be the weakest binder. The ligand of 1EXX is an inactive stereoisomer of the 1EXA ligand.³⁶ The calculated binding free energy for the 1EXX ligand is not included in Figure 4, because no experimental value is available. Overall, a good LIE model is obtained for both cases with RMS errors of 0.7 and 0.9 kcal/mol for simulations starting from crystal structure conformations and docked conformations, respectively. This indicates that the LIE method can indeed be used for binding free energy predictions of docked compounds for this system.

Comparison of LIE Models and Scoring Functions. MMP3, ER α , and DHFR were used to evaluate the LIE method with large sets of ligands for each target. The proteins

Table 2. Performance of the Best LIE Model for Each System^a

target	LIE								
	α	β	δ	R^2 training set	RMS error training set	RMS error test set	Spearman rank training set	Spearman rank test set	Spearman rank total
RAR γ xray	0.42	0.35		0.81	0.74				
RAR γ dock	0.42	0.41		0.70	0.92				
MMP-3	0.38	0.066	0.14	0.33	0.88	1.0	0.68	0.50	0.59
ER α	0.76	0.24	0.24	0.87	0.63	1.3	0.89	0.60	0.65
DHFR Otzen	0.42	0.083	-0.30^b	0.20	0.85	0.81	0.090	0.27	0.054
			0.18 ^c						
DHFR Zolli-Juran	0.42	0.083	-0.30^b			1.7		0.49	0.49
			0.18 ^c						

^a The best models were selected on the basis of the RMS errors from the experimental binding free energies. The RMS error is given in kcal/mol. The Spearman rank correlation coefficient is also shown. α , β , and δ correspond to the coefficients of the LIE model, eq 5. "xray" and "dock" for RAR γ correspond to MD simulations using crystallographic and docked conformations as starting structures, respectively. The RAR γ data set was not divided into training and test sets. ^b Coefficient of the ligand–ligand intramolecular van der Waals interaction energy. ^c Coefficient of the ligand–ligand intramolecular electrostatic interaction energy. For DHFR, the LIE models are trained on the training set of the Otzen compounds and the Zolli-Juran compounds are used as an additional external test set.

have diverse binding site properties, representing different target classes. The ligand set for each target originates from the same chemical series and displays a range from low nanomolar to micromolar binders, thus representing realistic lead optimization test cases for LIE model validation. The three ligand sets were divided into training and test sets of equal size and range in binding affinity. The LIE models were parametrized using the training sets and validated with the test sets. Similarly, a linear regression between scoring functions and binding affinities was performed on the basis of the training set, which was subsequently used to predict affinities from scores for the test sets.

MMP-3. The active site of MMP-3 is located in a large cleft, open toward the solvent. Matrix metalloproteases display a catalytic zinc ion coordinated by three histidine residues and a water molecule, which is displaced by the ligand in inhibitor complexes (see Figure 2).⁴⁹ A total of 54 ligands²³ were docked to the 1HY7 crystal structure.²⁷ All compounds contain a carboxylic acid coordinating the zinc ion and a biphenyl moiety as P1' substituents. The ligands mainly differ on the P2 side, where the molecules are fairly flexible and bind in the large, lipophilic, open part of the active site, S2. The ligand of the crystallographic complex (1HY7) also contains a carboxylic acid and a biphenyl group. The 1HY7 ligand and the two scaffolds of the MMP-3-inhibitor set are displayed in Figure 1. The carboxylic acid interacts with the zinc ion in a bidentate fashion, and the biphenylic group fits into the partly closed S1' pocket, as displayed in Figure 2.²⁷ The binding mode of the 1HY7 compound could thus be used to guide the selection of docking poses for the data set. The docking solutions all displayed the strong electrostatic interaction between the zinc ion and the ligand carboxylic acid, placing the biphenyl group in the S1' pocket. The position of the P2 part of the molecules was more varied among the data set, the binding pocket being larger and open toward the solvent on this side.

LIE models constructed on the basis of eq 2 did not give satisfying free-energy predictions or ranking of the ligands of the data set (RMS error for the training and test sets are 0.99 and 1.2 kcal/mol, respectively; Spearman rank correlation coefficients were 0.53 and 0.43 for the training and test sets, respectively). The parametrization of eq 5 for the MMP-3 data set resulted in improved, more predictive

models. Introducing a constant γ , as in eq 3, did not improve the models but resulted in a poorer ranking of the ligands (RMS errors for the training and test sets were 0.89 and 1.0 kcal/mol, respectively, and Spearman rank correlation coefficients were 0.56 and 0.38 for the training and test sets, respectively). Likewise, using different values for β_{prot} and β_{wat} and for α_{prot} and α_{wat} did not increase the quality of the models. The results of the LIE model compared to the results of the best performing scoring function are displayed in Figure 5 and Tables 2 and 3. The β value of the MMP-3 model is very low, because of the large electrostatic energy difference between the protein and water simulations. This can be traced down to the strong electrostatic interaction between the carboxylic acid of the ligands and the zinc ion in the protein. Even with the low β , the contribution to the total binding free energy is approximately -4 kcal/mol, that is, about half of the calculated binding free energy. The RMS error from the experimental values is 0.9 and 1.0 kcal/mol for the training and test sets, respectively.

The best performing scoring function, HM-Score, shows a low RMS error (0.8 kcal/mol) for the training set but an RMS error of 1.1 kcal/mol for the test set. The ranking of the test set is also significantly worse than that of the LIE model, as can be seen in Figure 5 and from the Spearman rank correlation coefficients in Tables 2 and 3. The Spearman rank correlation coefficient for the test set of HM-Score is as low as 0.17. A large number of the compounds in the test set are predicted to have approximately the same binding free energy by HM-Score, while the LIE model better distinguishes the differences between the compounds.

Because of difficulties in the parametrization of the zinc ion, different parameters for the zinc ion and its coordination bonds were tested. This did not result in significant differences in the final LIE model. Because of the similar nature of the ligands, any errors due to the parameters of the zinc ion are likely to be canceled out during the parametrization of the LIE model.

ER α . The binding site of ER α is a closed pocket, mainly consisting of hydrophobic residues. The native ligand, 17 β -estradiol, is anchored at one end of the pocket through a hydrogen-bond network to Arg394, Glu353, and a water molecule. His524 on the opposite side of the cavity offers additional ligand anchoring through hydrogen bonding as

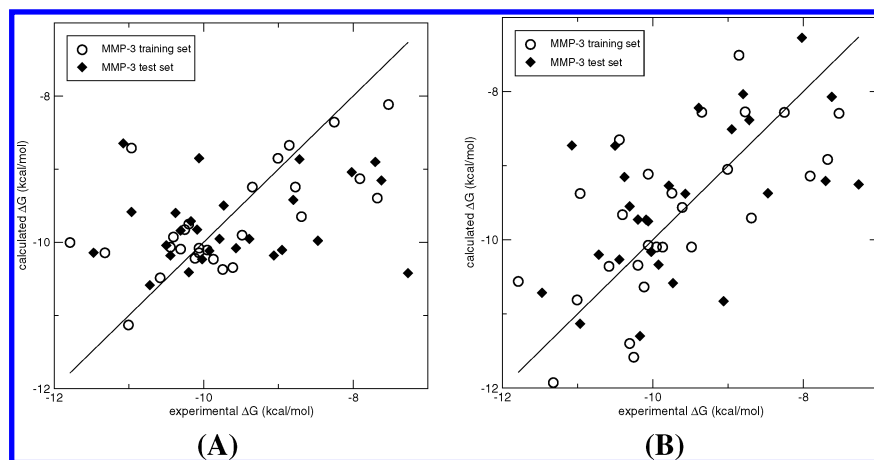


Figure 5. Comparison between the best performing scoring function, HM-Score (A), and the LIE model (B) for the MMP-3 ligand set; experimental binding free energies are compared to predicted binding free energies. The models were constructed using a training set and validated with an external test set. The solid line represents the ideal case.

Table 3. Performance of the Best Scoring Function for Each System^a

target	best scoring function	Scoring					
		R^2 training set	RMS error training set	RMS error test set	Spearman rank training set	Spearman rank test set	Spearman rank total
MMP-3	HM-Score	0.43	0.81	1.1	0.57	0.17	0.38
ER α	HS-Score	0.62	1.05	1.54	0.52	0.54	0.55
DHFR Otzen	HP-Score	0.37	0.72	0.67	0.45	0.44	0.35
DHFR Zolli-Juran	HP-Score			1.6		0.064	0.064

^a The best models were selected on the basis of the RMS errors from the experimental binding free energies. The Spearman rank correlation coefficient is also shown. The RMS error is given in kcal/mol. For DHFR, the scoring models are trained on the training set of the Otzen compounds and the Zolli-Juran compounds are used as an additional external test set.

displayed in Figure 2.²⁸ A total of 36 compounds with known binding affinities²⁴ were docked to the ligand-binding domain of ER α (IERE).²⁸ The compounds are all fairly rigid, including an aromatic group corresponding to the A ring of estradiol. A number of the compounds have several hydroxyl groups offering additional hydrogen-bond possibilities, for example, to His524, see Figure 2. For one of the ligands, no docking solution could be obtained, probably because of induced fit, requiring the protein atoms to rearrange to accommodate the ligand. As for MMP-3, the extended LIE model described by eq 5, taking the ligand intramolecular interactions into account, resulted in the best model. The parametrization of the LIE model resulted in the identification of two outliers in the training set, with an error of more than 2 kcal/mol. Mimicking a real case scenario, these two compounds were excluded from the set and the LIE model was reparametrized with the remaining compounds of the training set. For the best performing scoring function, HS-Score, these compounds were not distinguished as outliers and were thus included in the training set. The resulting LIE model performs reasonably well, as displayed in Figure 6 and Tables 2 and 3, with an RMS error of the test set of 1.3 kcal/mol.

Stereoisomers displaying large differences in binding free energy, ranging from good (−13 kcal/mol) to intermediate (−11 kcal/mol) binders, constitute a challenge within the ER α data set. The stereoisomers only differ in the direction of an alkyl chain attached to the chiral center (compare Figure 1, ER α scaffold 1);²⁴ that is, the differences in binding affinity do not originate directly from less favorable electrostatic interactions but mostly from the van der Waals

contribution. The less favorable binding free energy could also partly be due to an inability to form the hydrogen bond with His524 in order to accommodate the alkyl chain in the cavity.

To optimize the LIE model, simulations from alternative docking poses were considered. These revealed differences in observed interactions between different docking poses of single compounds and between different compounds. Another approach for LIE model construction was therefore tested. The data set was divided into two groups depending on the binding mode, and different LIE models were obtained for both groups. This resulted in an improved overall model with considerably improved ranking and RMS errors of 0.8 and 0.9 kcal/mol for the training and test sets, respectively (data not shown). However, the required visual inspection and grouping of the binding modes decreases the high-throughput nature of the method. It illustrates the difficulty of evaluating docking solutions efficiently and the inaccuracy introduced by the first, docking, step of the proposed method.

Both the original LIE model and the modified two-group model perform better than the best performing scoring function, HS-Score, in terms of the RMS error of the test set and are also better in ranking of the compounds. The RMS error of the training set of HS-Score is 1.1 kcal/mol, but the corresponding value for the test set is as high as 1.5 kcal/mol, consistent with what was observed for the scoring results of MMP-3. Also, in terms of the Spearman rank correlation, the LIE model performs better than the scoring function.

DHFR. DHFR catalyzes the NADPH-dependent reduction of dihydrofolate to tetrahydrofolate. The target structure

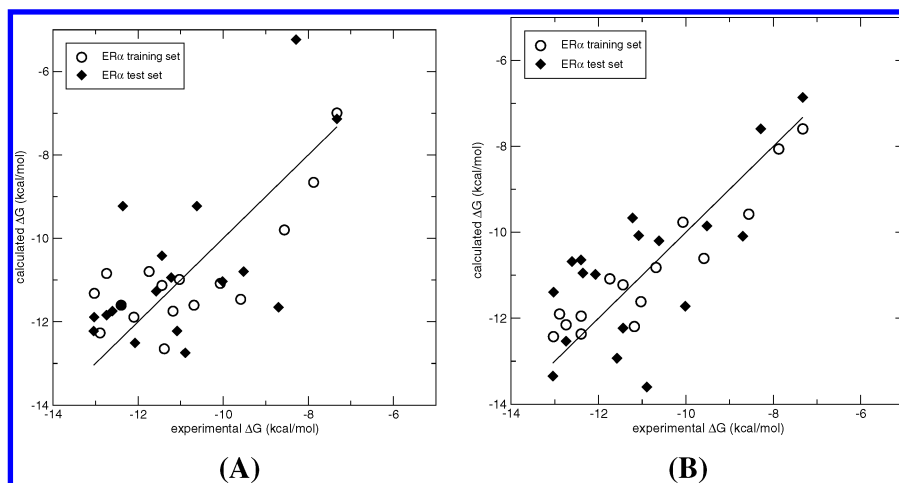


Figure 6. Comparison between the best performing scoring function, HS-Score (A), and the LIE model (B) for the ER α ligand set; experimental binding free energies are compared to predicted binding free energies. The models were constructed using a training set and validated with an external test set. Two outliers ($|\text{error}| > 2$ kcal/mol) were excluded from the training set when the LIE model was constructed. These outliers are not shown in the figure. The solid line represents the ideal case.

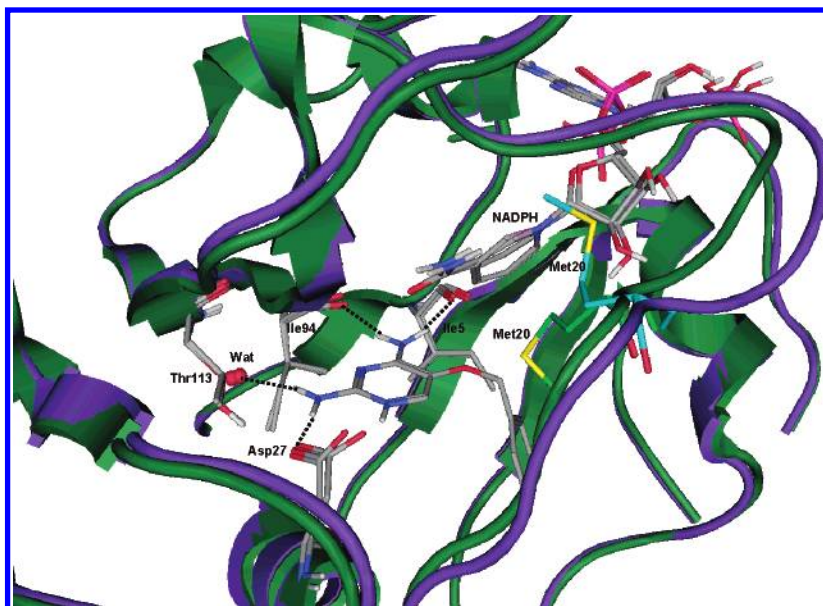


Figure 7. Comparison of the active sites of two DHFR crystal structures, 1RX3 (green) and 1RA2 (blue). The Met20 loop is shifted in 1RA2, and Met20 (cyan) is rotated upward compared to Met20 in 1RX3 (green). The suggested binding mode of the diaminopyrimidine ligands is indicated in gray. The charged nitrogen of the ligand is interacting with Asp27.

1RX3²⁹ was used for all docking and MD calculations. 1RX3 is the cocrystal structure of *Escherichia coli* DHFR, NADPH, and methotrexate (MTX). The binding pocket is made up of a tight, elongated, hydrophobic cavity, approximately 9 Å deep. A well-defined hydrogen bonding pattern is located at its bottom, accommodating the diamino-pteridine part of MTX, displayed in Figure 1. The hydrophilic solvent-exposed cleft accommodates the para-amido diacid phenyl part of MTX. The diamino-pteridine head makes four hydrogen bonds to the enzyme (compare Figure 7): one primary amine donates one hydrogen bond to Asp27 and one to a water molecule, which makes three additional hydrogen bonds to protein residues. The other primary amine donates one hydrogen bond to the backbone carbonyl of Ile5 and one to the backbone carbonyl of Ile94. Further, one pteridine ring nitrogen is located at 2.3 Å from Asp27 and is, hence, modeled as positively charged. The known actives were collected from two sources, one set of 29 compounds being close analogues from the same structure–activity relationship

series,²⁵ referred to as the Otzen compounds, and one set of 11 compounds from a high-throughput screen,²⁶ referred to as the Zoll-Juran compounds. The experimental binding pose of MTX was used to guide the selection of docking poses of the known actives. The Otzen compounds all contain a diaminopyrimidine moiety. The scaffold of the compounds is displayed in Figure 1. The Otzen compounds were docked into the cavity with the protonated diaminopyrimidine in the same position as MTX, except for two compounds that do not reach all the way into the hydrophobic cavity, not forming the same hydrogen-bonding pattern as the other compounds. Seven of the Zoll-Juran compounds contain a diaminopyrimidine moiety (or tetrahydrodiaminopyrimidine) as displayed in Figure 1; one contains diaminotriazine, one contains thiobisguanidine, one contains bisguanidine, and one lacks a basic nitrogen. Most Zoll-Juran compounds also docked to form the ionic hydrogen bond with Asp27, but the triazine-containing compound and the compound lacking a basic nitrogen did not form the described MTX hydrogen

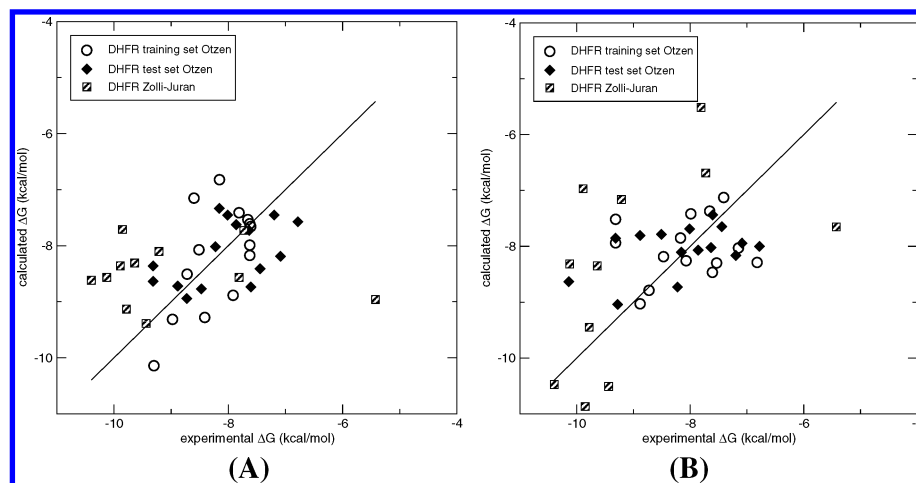


Figure 8. Comparison between the best performing scoring function, HP-Score (A), and the LIE model (B) for the DHFR ligand set; experimental binding free energies are compared to predicted binding free energies. The models were constructed using a training set of the Otzen compounds and validated with an external test set. An additional test set consisting of the Zolli-Juran compounds is shown in blue. The solid line represents the ideal case.

bonds. The docking poses of these compounds as well as the nonstandard bisguanidine-containing compounds can be considered to be relatively uncertain. The diaminopyrimidine or a diaminoquinazoline moiety, which most known actives contain, was modeled as positively charged in order to make the ionic hydrogen bond to Asp27 as observed for MTX.

The best performing LIE model constructed and tested on the Otzen compounds was again obtained including the intramolecular ligand interaction (eq 5). Weighting the van der Waals and electrostatic contributions of the ligand intramolecular interactions differently was necessary, as described in eq 4. Results of the LIE model are shown in Table 2 and Figure 8. No well-performing LIE model could be obtained for the DHFR Otzen compounds. Although the RMS errors are relatively low, 0.8 kcal/mol for both the training and test sets, the ranking of the compounds is generally poor, which is shown in Figure 8 and by the Spearman rank correlation coefficient of 0.054. β is decreased to become insignificantly low, contributing typically +1 kcal/mol to the binding free energy. This indicates that there is no correlation between the electrostatic interactions and the value of ΔG_{bind} . The van der Waals contribution of the intramolecular ligand interactions is also weighted negatively in the LIE model. The best performing scoring function, HP-Score, yields similar results for the Otzen compounds, displaying relatively low RMS errors but poor ranking, although the results are better than those of the LIE model, with a Spearman rank correlation of 0.35, see Table 3. The LIE model parametrized on the training set of the Otzen compounds²⁵ applied to the Zolli-Juran compounds²⁶ does not give satisfactory predictions, with an RMS error of 1.7 kcal/mol. The scoring of these compounds gives similar results, but the ranking of the Zolli-Juran compounds is significantly better in the LIE model, as can be seen from the Spearman rank correlation coefficients of 0.49 for the LIE model and 0.064 for HP-Score. The Zolli-Juran compounds displaying the relatively uncertain docking poses described above are generally outliers in the LIE model, while they obtain approximately the same docking score as the other compounds, see Figure 8. One reason for the relatively poor quality of the DHFR LIE model is that the range of experimental binding affinities is rather small, ~ 3

kcal/mol. This is reflected by the fact that reasonable RMS errors are obtained for both the LIE model and the best scoring function predictions but the Spearman rank correlation coefficients and the correlation with experimental data is particularly poor. We further suggest that the reasons for the inaccuracies in describing this system could lie in the docking of the compounds, where problems of induced fit have been observed previously⁵⁰ involving conformational changes in the Met20 loop near the cofactor,²⁹ see Figure 7. Another possible source of error is the protonation state of the diaminopyrimidines, because the low β values suggest the inaccuracies stem from the electrostatic interaction energies. However, protonation of the diaminopyrimidines seems necessary to anchor the ligands in the active site during docking. The parametrization and description of the interactions with the NADPH may also be a source of error.

DISCUSSION

The comparison between the LIE models obtained by using crystal structure ligand conformations and docked ligand conformations as starting structures for MD showed that the LIE models perform similarly in the case of RAR γ , where the docking solutions were considered to be good. However, as was shown for DHFR, the applicability of the LIE method will depend on the docking performance to the target of interest. Major conformational changes upon ligand binding will not be accounted for by the relatively short molecular dynamics simulations used in this approach.

In a study of binding affinity estimation of metalloprotease (MMP) ligands of Khandelwal et al.,⁵¹ a rigorous four-step approach was applied, including docking, subsequent QM/MM optimization of the complex followed by molecular dynamics simulation and LIE calculations, and single-point QM/MM energy calculation of the obtained time-averaged structures. In this study, the solvent-accessible surface area is included as a term in the LIE equation (eq 3).⁵² In our approach, we did not need to include the solvent-accessible surface area as a term in the LIE equation but did include the differences in ligand–ligand intramolecular interactions to improve our model, which could account for similar corrections. The obtained weight for the electrostatic term,

β , is either negative or omitted completely in the different suggested LIE models of the Khandelwal study, which is reminiscent of the very low β we observe, although the low β values still result in a significant contribution to the binding free energies in our study. Although difficult to compare quantitatively, the results of our MMP-3 study are of similar quality as those of the first three steps of the Khandelwal et al. study (RMS error of 0.5–0.7 kcal/mol, without using an external test), considering the larger size of our complete data set as well as the test set size of 27 compounds. No QM/MM optimization of the docked compounds needed to be performed to achieve this. QM/MM interaction energy calculations of the time-averaged structures in the Khandelwal et al. study decrease the RMS errors. Apart from the fact that one can doubt the physical relevance of a time-averaged structure as representative of an entire ensemble, the extra cost both computationally and in human time for data analysis render this approach inapplicable for a high-throughput setup. In terms of ranking the compounds, the LIE model we describe also performs satisfactorily.

The LIE models for MMP-3 and ER α perform better than the best performing scoring function, selected from a set of 10 scoring functions. For DHFR, the predictions from the LIE model are as equally poor as those of the best scoring function. For both MMP-3 and ER α , two systems with diverse properties, the ranking of compounds by the LIE model is superior to the ranking by the best scoring function, according to the Spearman rank correlation coefficient. Accurate ranking according to binding affinity of a set of similar ligands is a particularly important factor in lead optimization. The LIE model RMS errors of the test sets range from 0.8 to 1.3 kcal/mol (1.7 kcal/mol if the DHFR Zolli-Juran set is included). Using the LIE model to refine docking solutions and obtain a more accurate prediction of the binding affinity seems to be a possible alternative to applying scoring functions only.

To realistically apply this approach in structure-based drug design, in particular in the pharmaceutical industry, the computational cost and required time for setup and analysis are important factors. In our study, we used simulation times of 350–500 ps, which corresponds to approximately 6 h per ligand simulation on a 2.0 GHz Intel Xeon processor. Two simulations are performed per ligand, which is easily parallelized. We estimate that up to 20 compounds could be evaluated by the method in 6 h on commonly available computer clusters of 40 nodes. This renders the LIE method not suitable for a virtual screening approach, involving thousands of compounds, but could be a useful tool in lead optimization, working with fewer and more similar compounds. We have devised an automated setup which can be used after manual protein preparation and initial calibration of the LIE model. These steps can be elaborate and require good knowledge of the binding site. Docking poses need to be inspected, and proper knowledge of important ligand–protein interactions is needed, important in any lead optimization program. However, the manual protein setup and initial calibration of the LIE model has to be carried out only once for every target. After this, the method can be used in a more automated fashion to predict ligand binding affinities for new compounds starting from docked poses.

Our study has shown that applying the LIE method is not as straightforward as simply using the original LIE equation

(eq 2), but improved models can be obtained including different terms, for example, the intramolecular interaction energies, for each system. The LIE method thus requires a number of binders with known binding affinity to parametrize the model and an analysis of the obtained interaction energies of the training set in order to construct the best performing LIE model for that particular system. With more experimental data available, the model can also be stepwise refined. Similarly, finding the best performing scoring function for the system of interest, as is currently suggested in the literature,^{2,5,6} seems as elaborate a task.

In summary, it seems possible to apply the LIE method in a lead optimization program, although the quality of the predictions depends on the target of interest, as well as on the docking performance to that target and the quality and amount of experimental data available. The experiences obtained with the system at the setup and model calibration stage seem to give a good indication as to the quality of the predictions of the test set. In our study, reasonable docking poses and LIE models were obtained for the training sets of MMP-3 (Spearman rank correlation coefficient: 0.68), which resulted in similarly well-performing models for the test set (Spearman rank: 0.50), while the less reliable docking poses and poor ranking of the training set of DHFR (Spearman rank: 0.09) resulted in a bad ranking of the test set for this system (Spearman rank: 0.27). In contrast, obtaining a good regression for the scoring functions does not lead to predictive test set models, as was shown for MMP-3, where the Spearman rank correlation coefficient drops from 0.57 for the training set to 0.17 for the test set. Generally, as an addition to the simple docking/scoring approach, molecular dynamics simulations and LIE calculations can give valuable information about the system in terms of solvation effects, flexibility, and ligand strain. In addition, improved predictions of binding affinities are obtained at a computational cost which is certainly affordable with modern computational resources and software.

CONCLUSIONS

The possibilities to apply the linear interaction energy method¹² in lead optimization programs was explored using four real-case examples with publicly available reference data. An automated setup was constructed to perform molecular dynamics simulations and LIE calculations from docked ligand–protein complexes. The LIE models were evaluated in terms of RMS errors with respect to the experimental values and by using the Spearman rank correlation coefficient. The results were compared to the best scoring function, which was selected from a set of 10 different scoring functions applied to the docking poses of the compounds.

The RAR γ example illustrates that good LIE models can be obtained from well-docked starting conformations, resulting in a model that is only slightly less accurate than a model obtained starting from crystal structure complexes.

Including a ligand–ligand interaction energy term in the LIE equation results in models for MMP-3 and ER α that perform better than the best scoring function both in terms of RMS errors and, in particular, in terms of ranking. The model for ER α could be further refined by dividing the compounds into two groups according to the docking pose,

although this restricts the applicability of the method in an automated manner. Even though reasonable RMS errors were obtained for the DHFR system, both scoring functions and the LIE method perform badly in terms of correlation with experimental values and the Spearman rank correlation. In part, this is attributed to the small range in experimental values and in part to differences in protein conformations for different compounds, which are not observed in the simulation time scale of this study.

The described method involves human effort and input at the initial stages of protein preparation and model construction but is automated for the prediction of binding affinities for a new ligand set. This makes application in lead optimization possible and also feasible considering currently available computational resources. Overall, the LIE method can be used as an addition to empirical scoring functions and docking experiments.

ACKNOWLEDGMENT

The authors thank prof. Johan Åqvist for making the Q program available. In addition, we thank him and co-workers, in particular, Martin Almlöf, for useful discussions.

Supporting Information Available: Ligand structures and the derivation of eq 4. This information is available free of charge via the Internet at <http://pubs.acs.org>.

REFERENCES AND NOTES

- Teague, S. J. Implications of protein flexibility for drug discovery. *Nat. Rev. Drug Discovery* **2003**, *2*, 527–541.
- de Graaf, C.; Pospisil, P.; Pos, W.; Folkers, G.; Vermeulen, N. P. E. Binding mode prediction of cytochrome P450 and thymidine kinase protein–ligand complexes by consideration of water and rescoring in automated docking. *J. Med. Chem.* **2005**, *48*, 2308–2318.
- Gohlke, H.; Klebe, G. Approaches to the description and prediction of the binding affinity of small-molecule ligands to macromolecular receptors. *Angew. Chem., Int. Ed.* **2002**, *41*, 2644–2676.
- Ferrara, P.; Gohlke, H.; Price, D. J.; Klebe, G.; Brooks, C. L., III. Assessing scoring functions for protein–ligand interactions. *J. Med. Chem.* **2004**, *47*, 3032–3047.
- Warren, G. L.; Andrews, C. W.; Capelli, A.-M.; Clarke, B.; LaLonde, J.; Lambert, M. H.; Lindvall, M.; Nevins, N.; Semus, S. F.; Senger, S.; Tedesco, G.; Wall, I. D.; Woolven, J. M.; Peishoff, C. E.; Head, M. S. A Critical Assessment of Docking Programs and Scoring Functions. *J. Med. Chem.* published online August 13, 2005, DOI: 10.1021/jm050362n.
- Jacobsson, M.; Karlen, A. Ligand Bias of Scoring Functions in Structure-Based Virtual Screening. *J. Chem. Inf. Model.* submitted for publication.
- Pan, Y.; Huang, N.; Cho, S.; MacKerell, A. D., Jr. Consideration of molecular weight during compound selection in virtual target-based database screening. *J. Chem. Inf. Comput. Sci.* **2003**, *43*, 267–272.
- van Gunsteren, W. F.; Berendsen, H. J. C. Computer simulation of molecular dynamics: Methodology, applications and perspectives in chemistry. *Angew. Chem., Int. Ed.* **1990**, *29*, 992–1023.
- Mezei, M.; Swaminathan, S.; Beveridge, D. L. Ab initio calculation of the free energy of liquid water. *J. Am. Chem. Soc.* **1978**, *100*, 3255–3256.
- Beveridge, D. L.; DiCapua, F. M. Free energy via molecular simulation: Applications to chemical and biomolecular systems. *Annu. Rev. Biophys. Chem.* **1989**, *18*, 431–492.
- Brandsdal, B. O.; Österberg, F.; Almlöf, M.; Feilerberg, I.; Luzhkov, V. B.; Åqvist, J. Free energy calculations and ligand binding. *Adv. Protein Chem.* **2003**, *66*, 123–158.
- Åqvist, J.; Medina, C.; Samuelsson, J. E. A new method for predicting binding affinity in computer-aided drug design. *Protein Eng.* **1994**, *7*, 385–391.
- Yang, J. M.; Chen, Y. F.; Shen, T. W.; Kristal, B. S.; Hsu, D. F. Consensus scoring criteria for improving enrichment in virtual screening. *J. Chem. Inf. Model.* **2005**, *45*, 1134–1146.
- Wang, R.; Lai, L.; Wang, S. Further development and validation of empirical scoring functions for structure-based binding affinity prediction. *J. Comput.-Aided Mol. Des.* **2002**, *16*, 11–26.
- Wang, R.; Lu, Y.; Wang, S. Comparative evaluation of 11 scoring functions for molecular docking. *J. Med. Chem.* **2003**, *46*, 2287–2303.
- Wang, R.; Lu, Y.; Fang, X.; Wang, S. An extensive test of 14 scoring functions using the PDBbind refined set of 800 protein–ligand complexes. *J. Chem. Inf. Comput. Sci.* **2004**, *44*, 2114–2125.
- Hansson, T.; Marelus, J.; Åqvist, J. Ligand binding affinity prediction by linear interaction energy methods. *J. Comput.-Aided Mol. Des.* **1998**, *12*, 27–35.
- Marelus, J.; Graffner-Nordberg, M.; Hansson, T.; Hallberg, A.; Åqvist, J. Computation of affinity and selectivity: Binding of 2,4-diaminopteridine and 2,4-diaminoquinazoline inhibitors to dihydrofolate reductases. *J. Comput.-Aided Mol. Des.* **1998**, *12*, 119–131.
- Graffner-Nordberg, M.; Marelus, J.; Ohlsson, S.; Persson, A.; Swedberg, G.; Andersson, P.; Andersson, S. E.; Åqvist, J.; Hallberg, A. Computational predictions of binding affinities to dihydrofolate reductase: Synthesis and biological evaluation of methotrexate analogues. *J. Med. Chem.* **2000**, *43*, 3852–3861.
- Ljungberg, K. B.; Marelus, J.; Musil, D.; Svensson, P.; Norden, B.; Åqvist, J. Computational modelling of inhibitor binding to human thrombin. *Eur. J. Pharm. Sci.* **2001**, *12*, 441–446.
- van Lipzig, M. M. H.; ter Laak, A. M.; Jongejan, A.; Vermeulen, N. P. E.; Wamelink, M.; Geerke, D.; Meerman, J. H. N. Prediction of ligand binding affinity and orientation of xenoestrogens to the estrogen receptor by molecular dynamics simulations and the linear interaction energy method. *J. Med. Chem.* **2004**, *47*, 1018–1030.
- Almlöf, M.; Brandsdal, B. O.; Åqvist, J. Binding affinity prediction with different force fields: Examination of the linear interaction energy method. *J. Comput. Chem.* **2004**, *25*, 1242–1254.
- Ha, S.; Andreani, R.; Robbins, A.; Muegge, I. Evaluation of docking/scoring approaches: A comparative study based on MMP3 inhibitors. *J. Comput.-Aided Mol. Des.* **2000**, *14*, 435–448.
- Sippl, W. Receptor-based 3D QSAR analysis of estrogen receptor ligands – Merging the accuracy of receptor-based alignments with the computational efficiency of ligand-based methods. *J. Comput.-Aided Mol. Des.* **2000**, *14*, 559–572.
- Otzen, T.; Wempe, E. G.; Kunz, B.; Bartels, R.; Lehwerk-Yvetot, G.; Hansel, W.; Schaper, K. J.; Seydal, J. K. Folate-synthesizing enzyme system as target for development of inhibitors and inhibitor combinations against *Candida albicans*—synthesis and biological activity of new 2,4-diaminopyrimidines and 4'-substituted 4-aminodiphenyl sulfones. *J. Med. Chem.* **2004**, *47*, 240–253.
- Zolli-Juran, M.; Cechetto, J. D.; Hartlen, R.; Daigle, D. M.; Brown, E. D. High throughput screening identifies novel inhibitors of *Escherichia coli* dihydrofolate reductase that are competitive with dihydrofolate. *Bioorg. Med. Chem. Lett.* **2003**, *13*, 2493–2496.
- Natchus, M. G.; Bookland, R. G.; Laufersweiler, M. J.; Pikul, S.; Almstead, N. G.; De, B.; Janusz, M. J.; Hsieh, L. C.; Gu, F.; Pokross, M. E.; Patel, V. S.; Garver, S. M.; Peng, S. X.; Branch, T. M.; King, S. L.; Baker, T. R.; Foltz, D. J.; Mieling, G. E. Development of new carboxylic acid based MMP inhibitors derived from functionalized propargylglycines. *J. Med. Chem.* **2001**, *44*, 1060–1071.
- Brzozowski, A. M.; Pike, A. C.; Dauter, Z.; Hubbard, R. E.; Bonn, T.; Engstrom, O.; Ohman, L.; Greene, G. L.; Gustafsson, J. A.; Carlquist, M. Molecular basis of agonism and antagonism in the oestrogen receptor. *Nature* **1997**, *389*, 753–758.
- Sawaya, M. R.; Kraut, J. Loop and subdomain movements in the mechanism of *Escherichia coli* dihydrofolate reductase: Crystallographic evidence. *Biochemistry* **1997**, *36*, 586–603.
- Åqvist, J.; Luzhkov, V. B.; Brandsdal, B. O. Ligand binding affinities from MD simulations. *Acc. Chem. Res.* **2002**, *35*, 358–365.
- Friesner, R. A.; Banks, J. L.; Murphy, R. B.; Halgren, T. A.; Klicic, J. J.; Mainz, D. T.; Repasky, M. P.; Knoll, E. H.; Shelley, M.; Perry, J. K.; Shaw, D. E.; Francis, P.; Shenkin, P. S. Glide: A new approach for rapid, accurate docking and scoring. 1. Method and assessment of docking accuracy. *J. Med. Chem.* **2004**, *47*, 1739–1749.
- Halgren, T. A.; Murphy, R. B.; Friesner, R. A.; Beard, H. S.; Frye, L. L.; Pollard, W. T.; Banks, J. L. Glide: A new approach for rapid, accurate docking and scoring. 2. Enrichment factors in database screening. *J. Med. Chem.* **2004**, *47*, 1750–1759.
- Schrödinger, LLC, New York, NY.
- ProteinDataBank. <http://www.rcsb.org>.
- Klaholz, B. P.; Mitschler, A.; Belema, M.; Zusi, C.; Moras, D. Enantiomer discrimination illustrated by high-resolution crystal structures of the human nuclear receptor hRARgamma. *Proc. Natl. Acad. Sci. U.S.A.* **2000**, *97*, 6322–6327.
- Klaholz, B. P.; Mitschler, A.; Moras, D. Structural basis for isotype selectivity of the human retinoic acid nuclear receptor. *J. Mol. Biol.* **2000**, *302*, 155–170.

- (37) Renaud, J. P. R. N.; Ruff, M.; Moras, D. Crystal structure of the RAR- γ ligand-binding domain bound to all-trans retinoic acid. *Nature* **1995**, *378*, 681–689.
- (38) Klaholz, B. P. R. J. P.; Mitschler, A.; Zusi, C.; Chambon, P.; Gronemeyer, H.; Moras, D. Conformational adaptation of agonists to the human nuclear receptor RAR γ . *Nat. Struct. Biol.* **1998**, *5*, 199–202.
- (39) Marelius, J.; Kolmodin, K.; Feierberg, I.; Åqvist, J. Q. A molecular dynamics program for free energy calculations and empirical valence bond simulations in biomolecular systems. *J. Mol. Graphics Modell.* **1998**, *16*, 213–225.
- (40) Kaminski, G. A.; Friesner, R. A.; Tirado-Rives, J.; Jorgensen, W. L. Evaluation and reparameterization of the OPLS-AA force field for proteins via comparison with accurate quantum chemical calculations on peptides. *J. Phys. Chem. B* **2001**, *105*, 6474–6487.
- (41) Berendsen, H. J. C.; Postma, J. P. M.; van Gunsteren, W. F.; DiNola, A.; Haak, J. R. Molecular-dynamics with coupling to an external bath. *J. Chem. Phys.* **1984**, *81*, 3684–3690.
- (42) Clark, R. D.; Strizhev, A.; Leonard, J. M.; Blake, J. F.; Matthew, J. B. Consensus scoring for ligand/protein interactions. *J. Mol. Graphics Modell.* **2002**, *20*, 281–295.
- (43) Tripos Inc., St. Louis, MO.
- (44) Rarey, M.; Kramer, B.; Lengauer, T.; Klebe, G. A fast flexible docking method using an incremental construction algorithm. *J. Mol. Biol.* **1996**, *261*, 470–489.
- (45) Jones, G.; Willett, P.; Glen, R. C.; Leach, A. R.; Taylor, R. Development and validation of a genetic algorithm for flexible docking. *J. Mol. Biol.* **1997**, *267*, 727–748.
- (46) Muegge, I.; Martin, Y. C. A general and fast scoring function for protein–ligand interactions: A simplified potential approach. *J. Med. Chem.* **1999**, *42*, 791–804.
- (47) Kuntz, I. D.; Blaney, J. M.; Oatley, S. J.; Langridge, R.; Ferrin, T. E. A geometric approach to macromolecule–ligand interactions. *J. Mol. Biol.* **1982**, *161*, 269–288.
- (48) Eldridge, M. D.; Murray, C. W.; Auton, T. R.; Paolini, G. V.; Mee, R. P. Empirical scoring functions: I. The development of a fast empirical scoring function to estimate the binding affinity of ligands in receptor complexes. *J. Comput.-Aided Mol. Des.* **1997**, *11*, 425–445.
- (49) Chen, L.; Rydel, T. J.; Gu, F.; Dunaway, C. M.; Pikul, S.; Dunham, K. M.; Barnett, B. L. Crystal structure of the stromelysin catalytic domain at 2.0 Å resolution: Inhibitor-induced conformational changes. *J. Mol. Biol.* **1999**, *293*, 545–557.
- (50) Paul, N.; Kellenberger, E.; Bret, G.; Muller, P.; Rognan, D. Recovering the true targets of specific ligands by virtual screening of the protein data bank. *Proteins* **2004**, *54*, 671–680.
- (51) Khandelwal, A.; Lukacova, V.; Comez, D.; Kroll, D. M.; Raha, S.; Balaz, S. A combination of docking, QM/MM methods, and MD simulation for binding affinity estimation of metalloprotein ligands. *J. Med. Chem.* **2005**, *48*, 5437–5447.
- (52) Carlson, H. A.; Jorgensen, W. L. An extended linear response method for determining free energies of hydration. *J. Phys. Chem.* **1995**, *99*, 10667–10673.

CI0601214